



Experimental analysis of micro-tubular solid oxide fuel cell fed by hydrogen

F. Calise^a, G. Restuccia^{a,*}, N. Sammes^b

^a DETEC-University of Naples Federico II, P.le Tecchio 80, 80125, Naples, Italy

^b Department of Metallurgical and Materials Engineering, Colorado School of Mines, 1500 Illinois Street, Golden, CO 80401, USA

ARTICLE INFO

Article history:

Received 5 June 2009

Received in revised form 29 July 2009

Accepted 3 August 2009

Available online 31 August 2009

Keywords:

SOFC

Micro-tubular

ABSTRACT

This paper analyzes the thermodynamic and electrochemical performance of an anode supported micro-tubular solid oxide fuel cell (SOFC) fed by hydrogen. The micro-tubular SOFC used is anode supported, consisting of a NiO and $Gd_{0.2}Ce_{0.8}O_{2-x}$ (GDC) cermet anode, thin GDC electrolyte, and a $La_{0.6}Sr_{0.4}Co_{0.2}Fe_{0.8}O_{3-y}$ (LSCF) and GDC cermet cathode. The fabrication of the cells under investigation are described, and an analysis of the different procedures with emphasis of the innovations with respect to traditional techniques. Such micro-tubular cells were tested using a test stand consisting of: a vertical tubular furnace, an electrical load, a galvanostast, gas pipelines, temperature, pressure and flow meters. The tests on the micro-SOFC were performed using hydrogen, to determine the cell polarization. A parametric study is also presented with the scope to analyze the variations of the thermodynamic and electrochemical performances of the cell in function of its operating temperature and fuel flow.

© 2009 Elsevier B.V. All rights reserved.

1. Introduction

Solid oxide fuel cells (SOFCs) are considered one of the most promising technologies for distributed power/heat production, due to their peculiarities, such as: high electrical and thermal efficiencies, low emissions, large availability of high temperature heat for cogeneration purposes, and good reliability [1,2].

SOFCs have been investigated since the 1970s, however they are very far from a real commercialization since a number of issues must still be solved [3]. Currently, a number of different SOFC configurations are under investigation, namely: tubular, planar, tubular high power density (HPD) and micro-tubular [2,3].

Nevertheless, SOFCs are still far from commercial availability, mainly due to problems such as: cost targets, operating life, system optimization and eventual integration with traditional devices in hybrid systems, aiming at maximizing the overall electrical efficiency [3].

Solid oxide fuel cell applications have long been limited by the necessity to operate at high temperatures, causing prolonged start up times and materials constraints, among other cost increasing constraints [1–3]. Considerably decreasing the operating temperature of SOFCs is necessary for efficient power production, specifically in mobile applications where start up time and materials cost is of increasing importance. Reducing the operating temperature of SOFCs below 650 °C can extend the lifetime of the SOFC stack, lower cost by allowing the use of metal materials, and

can decrease the degradation of SOFC and stack materials [4,5]. Tubular SOFC designs have been shown to be stable for repeated cycling under rapid changes in electrical load and in cell operating temperatures [6–8]. However, tubular SOFC capital costs are very high end significantly far from the target of 400 US\$ kW⁻¹, planned by SECA. This is mainly due to their low power density and to the materials to be used for a safe operation at the high temperatures typical of SOFC stacks. In this framework, micro-tubular SOFC's aim at solving both the problems affecting the typical tubular SOFC. In fact, their lower diameter and operating temperature promise to: (i) reduce capital costs; (ii) increase power density; (iii) increase thermal shock resistance; and (iv) reducing start-up and shut-down times. In fact, micro-tubular SOFCs have also been shown to be able to endure the thermal stresses associated with rapid heating up to operating temperatures [9,10]. In contrast to planar SOFC designs, when the diameter of the tubular SOFC is decreased, it is possible to design SOFC stacks for high volumetric power densities [1,11].

However, literature data dealing with thermal, electrical and electrochemical performance of micro-tubular SOFC's are scarce, since this is an emerging technology. Therefore, this paper aims at presenting a detailed experimental analysis conducted on micro-tubular solid oxide fuel cells. In particular, in this work anode supported micro-tubular SOFCs with a cermet anode of NiO and GDC (gadolinium doped ceria), a GDC electrolyte and a cathode in LSCF ($La_{0.6}Sr_{0.4}Co_{0.2}Fe_{0.8}O_{3-y}$), were considered. These cells were tested at operating temperatures ranging from 450 °C to 550 °C. Such experimental analysis was carried out at varying cell temperature and fuel flow, in order to assess the effects of these two parameters on the electrochemical performance of the cell. To this scope, a parametric study is also presented.

* Corresponding author.

E-mail address: giulio.restuccia@unina.it (G. Restuccia).

Nomenclature

A	cell active area (cm^2)
F	Faraday's constant ($96,439 \text{ C mol}^{-1}$ of electrons)
\tilde{g}	Gibbs specific molar energy (kJ kmol^{-1})
h	specific enthalpy (kJ kg^{-1})
\tilde{h}	specific molar enthalpy (kJ kmol^{-1})
i	current density (mA cm^{-2})
I	current (A)
\dot{n}	molar flow rate (mol s^{-1})
p	pressure (bar)
p_{ref}	reference pressure (1 bar)
p_{H_2}	hydrogen partial pressure (bar)
$p_{\text{H}_2\text{O}}$	steam partial pressure (bar)
p_{CH_4}	methane partial pressure (bar)
P_d	power density (W cm^{-2})
\bar{R}	molar gas constant ($8.31 \text{ kJ kmol}^{-1}$)
t	temperature ($^{\circ}\text{C}$)
T	temperature (K)
U_f	fuel utilization factor
V	cell voltage (V)

Greek symbol

η_{el}	DC electrical efficiency
--------------------	--------------------------

2. Experimental

2.1. Solid oxide fuel cells test stand

The performance of the fuel cells was analyzed using an in-house SOFC test stand. Such stand is based on a *Carbolite vertical tubular Furnace* which is equipped with an advanced set-point programming temperature controller (power feedback is used to stabilize the output power and hence the controlled temperature against supply voltage fluctuations) and ramp rate temperature control, especially important for fuel cell testing in order to avoid possible rupture for thermal stress during start-up and shut down procedures. A ramp rate of $1.5\text{--}2.0^{\circ}\text{C min}^{-1}$ was used both for heat-up and cool down of the fuel cell.

The stand is also equipped with a *Chroma 6310 series Electrical Load*. This system is capable of drawing a fixed amount of current from the fuel cell and thus measuring the corresponding output voltage, both under static and dynamic condition. In addition, a *Gamry 600 Potentiostat/Galvanostat* was employed in order to evaluate and determine the typical EIS (electrochemical impedance spectroscopy) shape. Such component, by applying a small sinusoidal voltage perturbation on the fuel cell, monitors the system's resultant current response, for different frequencies, and is able to determine the EIS shape. Impedance information was gained using a frequency range of $100 \text{ kHz--}0.2 \text{ Hz}$ with signal amplitude of 10 mV under open circuit conditions.

The test stand also includes hydrogen, carbon monoxide, carbon dioxide, methane and nitrogen pipe lines. Furthermore, a bubbler system for steam production is also included in the test stand. Each line is equipped with a MKS thermal mass flow meters (type 179) gas flow controller linked to a MKS mass flow controller (MFC) capable of setting the expected volume flow. Each line is linked to a single cylinder containing a different gas. On the top of each cylinder a pressure reducer (regulator) was installed in order to achieve values of pressure inside the pipes higher than the environmental one ($20 \text{ psi--}138 \text{ kPa}$).

Finally, a PC data acquisition system was used in order to control the instrument and save the data produced during the experiments.

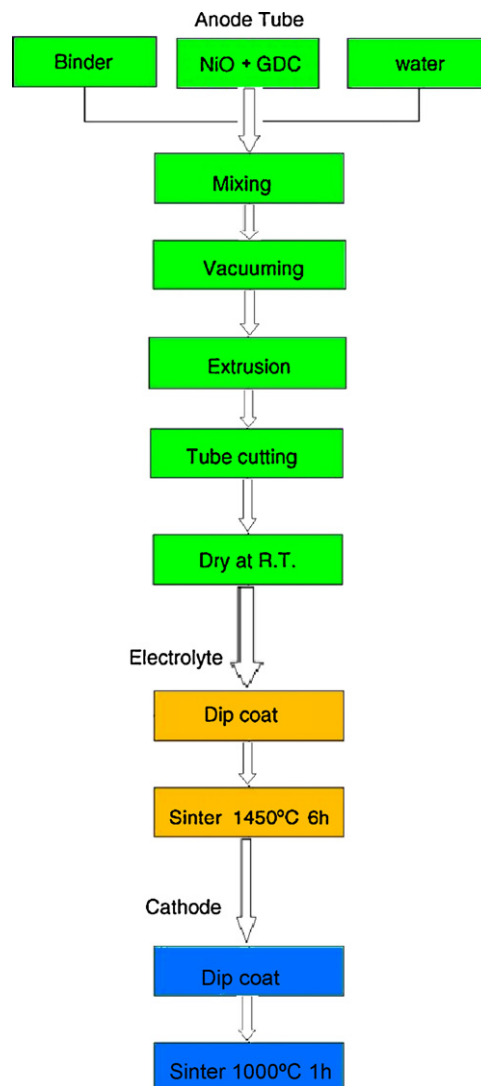


Fig. 1. Micro-tubular SOFC flow chart fabrication process.

2.2. Fabrication process

Micro-tubular SOFCs were developed with diameters in the millimeter and sub-millimeter ranges for intermediate temperatures operation between 450°C and 550°C [1,11,12]. In this study, micro-tubular SOFCs measuring 1.8 mm in diameter and 3.0 cm in length (with active cathode length of 8 mm , whose active cell area is estimated to be 0.45 cm^2) were fabricated. The micro-tubular SOFC used is anode supported, consisting of a NiO and $\text{Gd}_{0.2}\text{Ce}_{0.8}\text{O}_{2-x}$ (GDC) cermet anode, thin GDC electrolyte, and a $\text{La}_{0.6}\text{Sr}_{0.4}\text{Co}_{0.2}\text{Fe}_{0.8}\text{O}_{3-y}$ (LSCF) and GDC cermet cathode.

Micro-tubular SOFCs were fabricated using traditional extrusion and coating techniques in a process similar to that described by Suzuki et al. [12]. This process is briefly shown in Fig. 1 with changes to fabrication processes noted. Anode slurry was prepared and consisted of NiO powder, GDC powder, and cellulose as the binder. The anode components were mixed with DI-water using an industrial mixer for 1–2 h and left to age overnight. Placing a vacuum over the anode mixture allowed for excess air to be removed. Anode tubes were extruded from the anode mixture using a ram extruder and a custom made die. The anode tubes were allowed to dry, were cut to the desired length, then dip-coated in GDC electrolyte

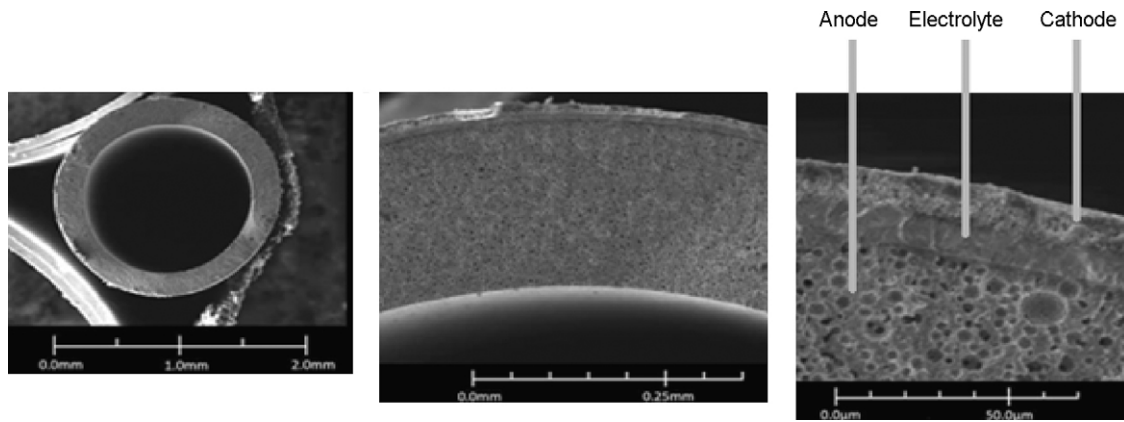


Fig. 2. SEM microstructure images of the micro-tubular SOFC.

slurry and allowed to dry. The GDC electrolyte slurry is composed of the same GDC powder described above, and organic ingredients such as binder (poly vinyl butyral), dispersant (fish oil) and solvents (toluene and ethanol). The desired electrolyte thickness was achieved through multiple electrolyte coatings and subsequently the tubes were sintered at 1450 °C for 6 h in air. Next, the electrolyte coated anode tubes were dip-coated in cathode slurry consisting of $\text{La}_{0.6}\text{Sr}_{0.4}\text{Co}_{0.2}\text{Fe}_{0.8}\text{O}_{3-y}$ (LSCF) and GDC powder, and organic ingredients similar with those of the electrolyte slurry. The cathode dip-coated tubes were dried in air and sintered at 1000 °C for 1 h in air to complete the fuel cell fabrication.

An environmental scanning electron microscope (ESEM) was used to check the electrode and electrolyte microstructure. Fig. 2 shows cross sectional ESEM images of the fabricated micro-tubular SOFC, with porous electrodes and a dense electrolyte.

In order to carry out the experimental activities, measuring the fuel cell electrochemical performance, a specific support was also manufactured. The support is capable of sustaining the fuel cell when it is mounted in the furnace, it also allows the gas distribution on the anode and cathode sides and assures the electrical connection with the electrical load and potentiostat. Each tube was connected to two alumina tubes allowing the inner anode gas distribution, sustaining the cell in the furnace. The entire system was placed on an alumina half tube support in order to yield a stronger structure (Fig. 3).

Fig. 4 shows how each micro-tube was mounted for testing within a vertically mounted micro-tube furnace (Carbolite). Cells were tested vertically as shown in Fig. 4 in order to ensure evenly distributed flow of fuel gas across the anode surface (horizontally oriented cells are subject to uneven fuel gas distribution due to gravity).

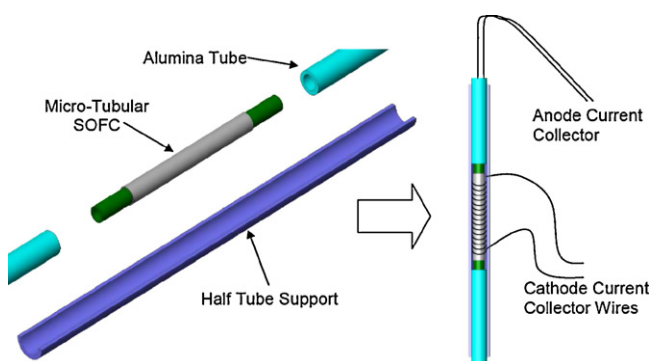


Fig. 3. Individual micro-tubular SOFC mount setup.

Each tube was equipped with four 0.5 mm silver sensor wires attached for collecting current for the anode and cathode sides. The anode electrical connection was realized using two long silver wires fixed using nickel paste. A silver wire was wrapped around the tubular fuel cell (on the cathode), as a reel, and fixed with silver paste for the cathode electrical connection. The silver paste and nickel paste were brush painted on the cathode and anode surfaces, respectively, to reduce the contact resistance between the silver sensor wires and the electrode surfaces. The pastes are porous enough at operating temperatures so that fuel and oxygen are able to pass through them to arrive at their respective electrodes. Ceramabond 552 (Aremco) was used as sealant between the anode, alumina tubes and alumina half tube support.

The four current collecting wires from the cell shown in Fig. 3 were connected to the impedance analyzer (Gamry 600) and the electrical load (Chroma 6310 series) at operating temperature ranges between 450 °C and 550 °C. Individual cells were run using humidified hydrogen gases (2–3% of H_2O) as a fuel to the anode side, while the cathode side (outside surface of tube) was exposed to atmospheric conditions. The type of air pump normally used for small aquariums was used to facilitate new air into the bottom of the micro-tube furnace to assist convective flow of air through the furnace.

The anode of the micro-tubular SOFC was maintained at 450 °C for 10 h before measurement of the I - V curve, power density curve and impedance information.

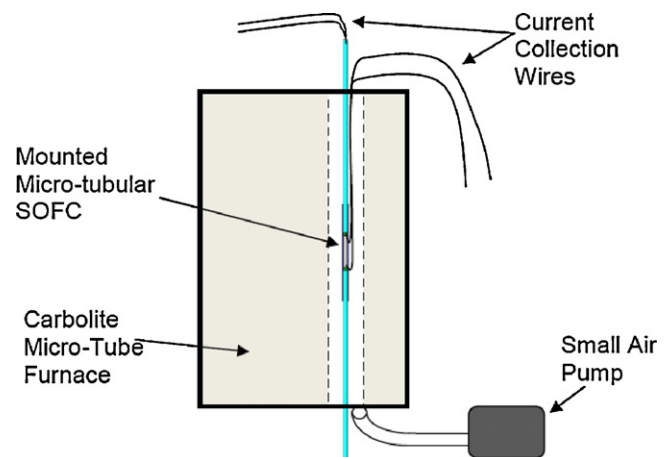


Fig. 4. Setup of micro-tubular SOFC inside of a vertical micro-tube furnace.

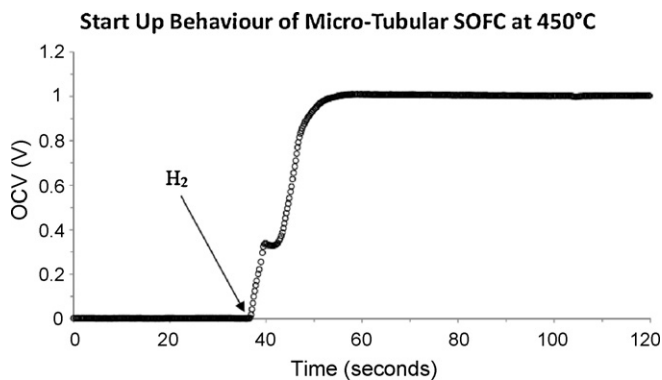


Fig. 5. Start-up behavior of the smaller micro-tubular fuel cell, reduced with N_2 and after fed with H_2 .

3. Results of the tests

3.1. Start up, OCV and ohmic resistance estimation

On the basis of the fabrication process described above different micro-tubular cells were realized. The cells used were 3 cm long (0.9 cm of reactive area length) with a 1.8 mm diameter for an active cell area of 0.5 cm^2 .

The start-up behavior of the smaller micro-tubular cell was investigated at 450°C and is shown in Fig. 5. For testing the start up behavior, the anode of the cell was fed with N_2 during the heating process, up to the selected operating temperature. When the temperature of 450°C was achieved, the cell anode was taken off N_2 and subjected to pure H_2 . The cell was able to be reduced in less than 1 min and reached an open circuit voltage (OCV) close to 1.0 V in that time.

The maximum performance of the smaller micro-tubular cell, fed by hydrogen, is shown in Fig. 6. The I - V (current density–voltage) curve and the power density curve shape are similar to the typical trends registered for others types of solid oxide fuel cells. The maximum power densities measured for this type of fuel cell were, respectively, 0.263 W cm^{-2} , 0.518 W cm^{-2} , and 1.310 W cm^{-2} at 450°C , 500°C , and 550°C , obtained at a fuel volume flow of $25 \text{ Scm}^3 \text{ min}^{-1}$ of H_2 (S , standard pressure and temperature, respectively, at 1.01325 bar and 15°C). These values show excellent power density performance, which significantly increases with the temperature: a variation of 100°C , increases the power density more than 1.000 W cm^{-2} (the value at 550°C is about 5 times higher than the corresponding value at 450°C).

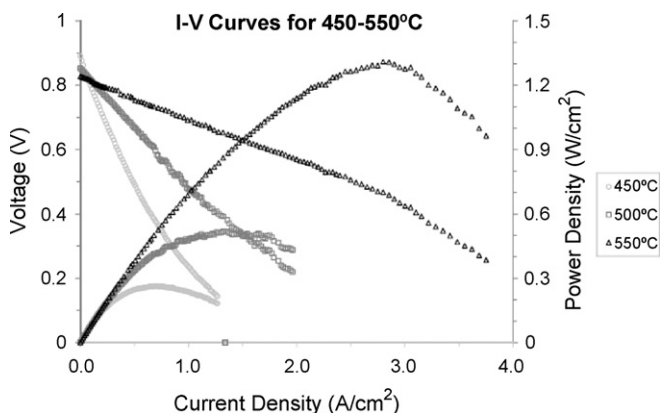


Fig. 6. I - V curves and power density curves for micro-tubular SOFC operating between 450°C and 550°C .

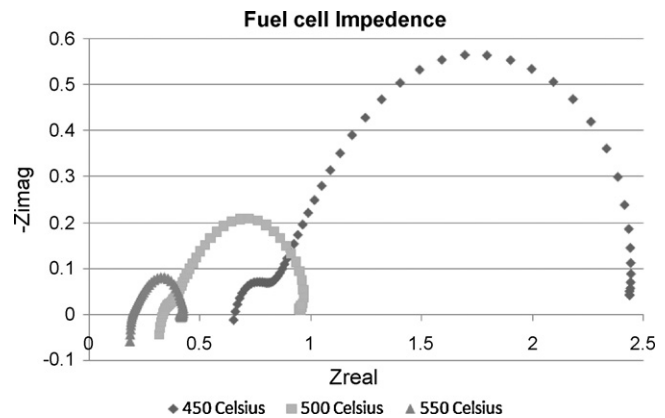


Fig. 7. Impedance spectroscopy of micro-tubular SOFC from 450°C to 550°C .

However, the OCV performance of the cell was somewhat lower if compared to the previous studies [11,12]. The OCV dropped from 0.892 V to 0.828 V as the temperature was increased from 450°C to 550°C . This drop in OCV can probably be explained by increases in electronic conductivity of the ceria electrolyte with increasing temperature in reducing environments.

The impedance spectra gathered from the micro-tubular SOFCs is shown in Fig. 7. The ohmic resistances of the micro-tubular cell were measured to be approximately 0.650Ω , 0.330Ω , and 0.200Ω at 450°C , 500°C , and 550°C , respectively. These measured resistances show improvement over resistances quoted in previous studies [11,12]. The reason for this improvement is likely due to decreased contact resistance obtained in this cell through careful preparation with silver and nickel pastes. The decreased contact resistance would lead to better current collection from the cell and the improved cell I - V performance confirms this notion.

Increasing the operating temperature, the shape of the impedance curve became smaller reducing both ohmic and activation polarizations. At 450°C it is possible to distinguish both the anodic and cathodic activation polarization curve represented by the two semi circles. At higher temperature the cathode impedance masks the impedance of the anode.

3.2. Effect of fuel flow rate and temperature

The sensitivity of the micro-tubular SOFC polarization curve as a function of its operating temperature fuel flow was investigated. To this scope, the fuel flow rate was varied from $1 \text{ Scm}^3 \text{ min}^{-1}$ to $25 \text{ Scm}^3 \text{ min}^{-1}$. Simultaneously, the operating temperature was varied from 450°C to 550°C , in order to assess the effect of this parameter on the cell performance.

The SOFC electrical performance was measured by the Chroma electric load over the range from open circuit voltage to 0.150 V. The minimum value of 0.150 V was used in order to avoid significant degradation in the fuel cells performance.

The electrochemical impedance spectroscopy was measured by galvanostat/potentiostat. Single cells were employed for these experiments. The cells used were 3 cm long (0.9 cm of reactive area length) with a 1.8 mm diameter for an active cell area of 0.500 cm^2 .

In general, the higher the fuel flow rate, the higher its electrical power. However, higher fuel flows would not necessarily determine higher efficiencies since this circumstance would also cause lower values of the fuel utilization factor. The effect of increasing hydrogen flow rate on the electrical power produced by a 0.500 cm^2 fuel cells, at different temperatures, is shown in the following figures (Figs. 8–10).

As expected, the graphs show an increase in power output with increasing fuel flow: at 550°C and for a fuel volume flow of

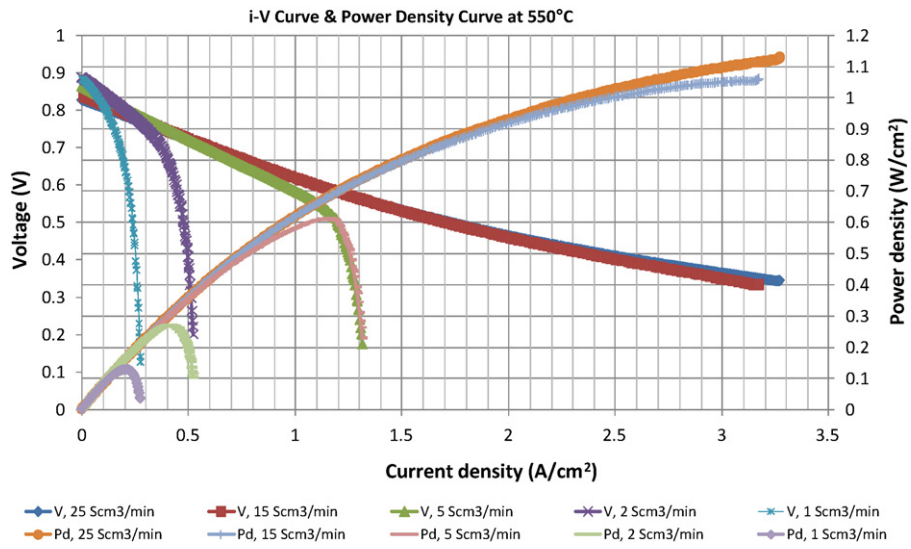


Fig. 8. Polarization and power density curves at 550 °C.

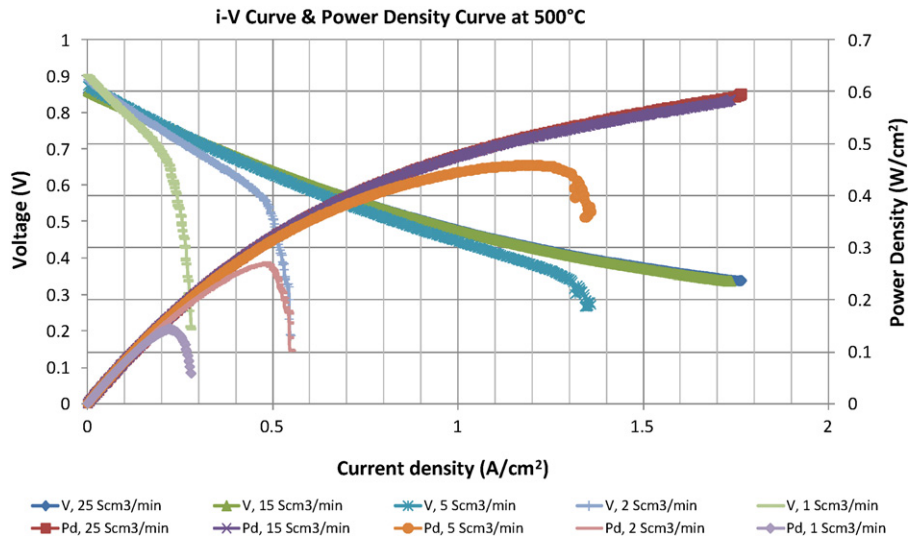


Fig. 9. Polarization and power density curves at 500 °C.

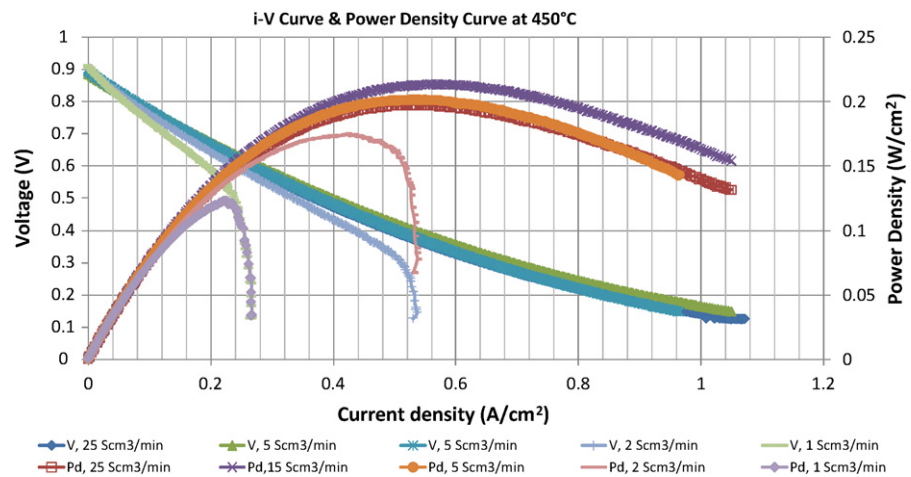


Fig. 10. Polarization and power density curves at 450 °C.

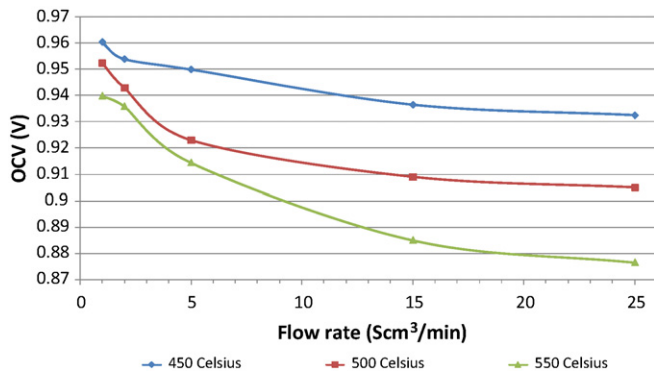


Fig. 11. OCV in function of operating temperature and fuel flow.

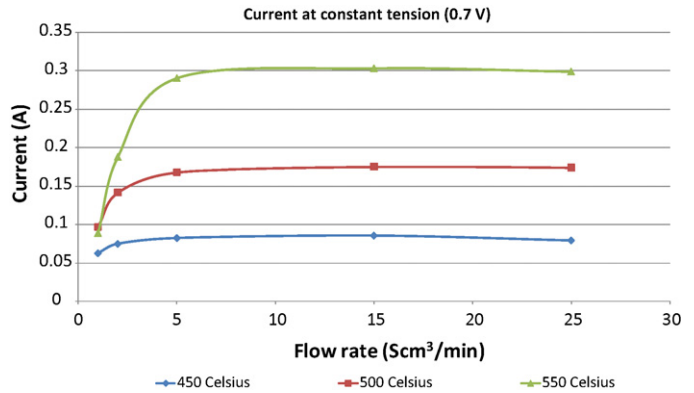


Fig. 12. Current (@ 0.70 V) in function of operating temperature and fuel flow.

$25 \text{ Scm}^3 \text{ min}^{-1}$ of H_2 , the maximum power density is 1.130 W cm^{-2} while, for a fuel volume of $1 \text{ Scm}^3 \text{ min}^{-1}$, the maximum power density is 0.130 W cm^{-2} , with a growth of almost one order of magnitude. The rate of increase fell off at the higher fuel volume flow. In fact the difference is less prominent between $15 \text{ Scm}^3 \text{ min}^{-1}$ and $25 \text{ Scm}^3 \text{ min}^{-1}$, while there is a greater difference between the maximum power density at $1 \text{ Scm}^3 \text{ min}^{-1}$, $2 \text{ Scm}^3 \text{ min}^{-1}$, $5 \text{ Scm}^3 \text{ min}^{-1}$ and $15 \text{ Scm}^3 \text{ min}^{-1}$.

Fig. 8 shows that at $15 \text{ Scm}^3 \text{ min}^{-1}$ and $25 \text{ Scm}^3 \text{ min}^{-1}$ the rate of decrease of both the I - V curve and power density curve are similar. Furthermore, at lower fuel flow rates, it is apparent that the effect of the concentration polarization, while at higher flow rates, the maximum current density is far from the anode and cathode limiting current density. Fig. 9 shows SOFC performance at 500°C while Fig. 10 reports the current density–voltage and current density–power density curves, evaluated at 450°C . The difference between the maximum power density measured at the highest and the lowest flow rate is 0.100 W cm^{-2} at 450°C while at 500°C it is 0.470 W cm^{-2} and at 550°C it is approximately 1.0 W cm^{-2} : Thus, increasing the temperature increases the difference in performance at different fuel flow rates. At higher temperature the electrochemical activity of the anode, cathode and especially the electrolyte increases increasing the internal surface area responsible for electrochemical reaction. For this reason, the fuel cell is more dependent on the changes in fuel flow rates. At 450°C , for hydrogen volume flow of $5 \text{ Scm}^3 \text{ min}^{-1}$, $15 \text{ Scm}^3 \text{ min}^{-1}$ and $25 \text{ Scm}^3 \text{ min}^{-1}$, both current density–voltage curves and current density–power density curves are similar. However, at 500°C only the curves at $15 \text{ Scm}^3 \text{ min}^{-1}$ and $25 \text{ Scm}^3 \text{ min}^{-1}$ are almost super-imposable. At 500°C , for $1 \text{ Scm}^3 \text{ min}^{-1}$, $2 \text{ Scm}^3 \text{ min}^{-1}$ and $5 \text{ Scm}^3 \text{ min}^{-1}$, is clearly shown the effect of the concentration polarization is clearly shown, while at 450°C , only for $1 \text{ Scm}^3 \text{ min}^{-1}$ and $2 \text{ Scm}^3 \text{ min}^{-1}$ this phenomena is clearly visible.

Fig. 11 shows the effect of temperature on the open circuit voltage for different values of the hydrogen volume flow and operating temperatures. As can be seen from the graph, the open circuit voltage has the expected downwards trend with temperature for all the different flow rates of fuel.

Looking at the Nernst equation for the hydrogen reaction:

$$E = \frac{\Delta g_f^0}{2 \times F} + \frac{\tilde{R} \times T}{2 \times F} \times \log \left(\frac{p_{\text{H}_2} \times \sqrt{p_{\text{O}_2}}}{p_{\text{H}_2\text{O}}} \right) \quad (1)$$

it can be seen that as the partial pressure of hydrogen is increased, E will be expected to increase. However, the experimental results show that the OCV trend is opposite to the Nernst equation indication. In fact for all the different temperature, the OCV became lower when the flow rate of hydrogen increased and this phenomenon is greater at higher temperature.

This phenomenon, opposite to the theoretical trend of the Nernst equation, could be explained with the fact that the electrolyte used in this cell is a ceria-based (GDC) oxide ion conductor. This material could lead to electronic conductivity and electronic current could flow through the electrolyte even at open circuit, with the result that the final voltage is somewhat lower than the theoretical value. The greater difference measured on the OCV at 550°C , for different hydrogen volume flow, compared with the values at 450°C , seems to confirm this possibility, with greater electronic conductivity of the ceramic materials at higher temperature.

It is also well known that the H_2 entering the cell could not completely be consumed in the stack. The ratio between the hydrogen reacted in the cell and that one entering the cell is the usual fuel utilization factor.

$$U_f = \frac{\dot{n}_{\text{H}_2, \text{reacted}}}{\dot{n}_{\text{H}_2, \text{in}}} \quad (2)$$

The current produced in an electrical system is directly related to the numbers of electrons involved. According to Faraday's law of electrolysis, $96,490 \text{ C}$ are produced per mole of electrons. In addition, the electrical efficiency is the ratio between the DC power produced by the cell and the potential energy included in the fuel reacted in the cell.

$$I = 2 \times \dot{n}_{\text{H}_2, \text{reacted}} \times F = 2 \times U_f \times \dot{n}_{\text{H}_2, \text{in}} \times F \quad (3)$$

$$\eta_{\text{el}} = \frac{V_{\text{cell}} \times I \times 10^{(-3)}}{\dot{n}_{\text{H}_2, \text{reacted}} \times |\Delta h_{\text{H}_2}|} = \frac{V_{\text{cell}} \times I \times 10^{(-3)}}{U_f \times \dot{n}_{\text{H}_2, \text{in}} \times |\Delta h_{\text{H}_2}|} \quad (4)$$

Oxygen ions carry two electrons per ion, therefore 1 mol of oxygen ions will produce $192,980 \text{ C}$. In turn, the amount of oxygen ions that can pass through a gadolinium doped ceria electrolyte depend on the temperature of the electrolyte as well as on the dopant level and thickness of the electrolyte. Thus, the amount of current produced by a tubular solid oxide fuel cell should increase with temperature. To investigate this, the current delivered by the cell is reported in Fig. 12; the current value was measured at 0.700 V for different temperature and different fuel flow rate.

The oxygen flux through a particular thickness of electrolyte is exponential with respect to temperature. As current is directly dependent on the flux of oxygen ions it would be expected that this should show a hyperbolic trend as the temperature of the fuel cell is increased. In fact the graph shows, as expected, an exponential relationship between increasing temperature and increasing current produced by the cell, but only for high flow rate (5 – 15 – $25 \text{ Scm}^3 \text{ min}^{-1}$).

It is possible that other factors are mitigating against the increase of ion flow, this includes an increase resistance within the current collection wires as the temperature is increased, and the

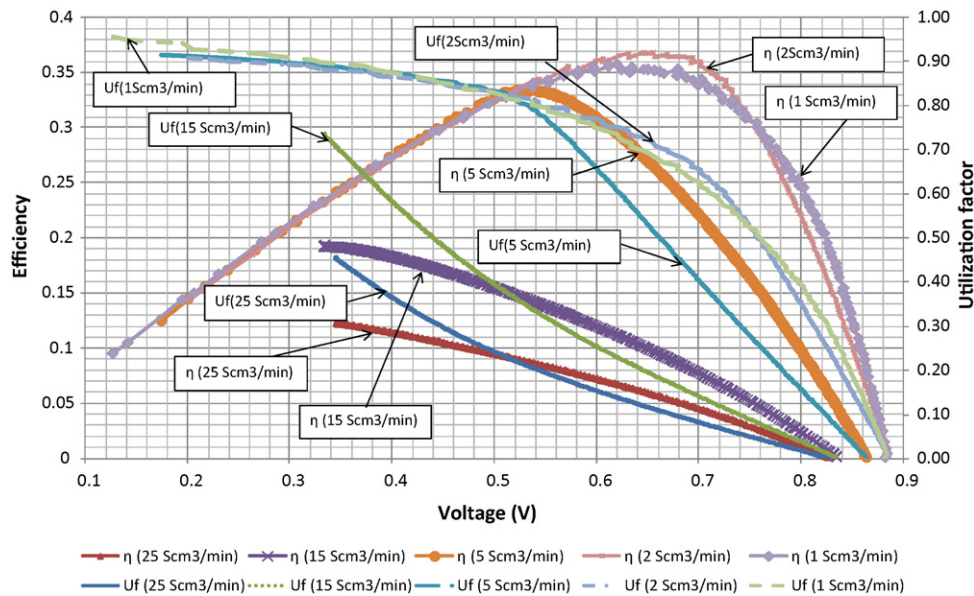


Fig. 13. Efficiency and fuel utilization factor varying cell voltage and fuel flow (@ 550 °C).

limiting effects of the kinetics of reaction. For example the amount of hydrogen adsorbed onto the catalytic surface may already be the limiting factor rather the oxygen flux through the electrolyte.

Fig. 13 shows the trend of the electrical efficiency and the fuel utilization factor, as a function of the fuel flow and operating voltage at the maximum allowable operating temperature (550 °C). Here, it is clearly shown that at the higher flow rates the lower electrical efficiency was observed. The maximum η_{el} is 12% at 25 Scm³ min⁻¹ and less than 20% at 15 Scm³ min⁻¹. At lower flow rates, the electrical efficiency and the fuel utilization is much higher: η_{el} is around 37% at 1–2 Scm³ min⁻¹ and 33% at 5 Scm³ min⁻¹, with fuel utilization factors, respectively, of 73% and 81%. Note that the maximum values of the electrical efficiencies are achieved for an operating voltage close to 0.660 V and the maximum value of the electrical efficiency is achieved for a fuel flow of 2 Scm³ min⁻¹. In fact, the lower the fuel flow, the lower the overvoltages occurring in the cell and the higher the amount of hydrogen reacted. This circumstance is also clear in the same figure, where the fuel utilization factor is higher at lower fuel flows. In addition, the fuel utilization factor is also significantly sensitive to the operating voltage. In fact, re-calling a typical polarization curve, the higher the voltage, the lower the current density, determining lower velocity of the electrochemical reaction and consequently causing a lower hydrogen conversion in the cell.

On the other hand, a maximum power density is obtained for higher fuel volume flow. Therefore, the selection of the optimal fuel flow depends on the selected objective function. The energetic efficiency can be maximized thus reducing that parameter. On the other hand, the economic profitability (power density) can be increased at higher operating fuel flows. It can be postulated that, the fuel flow rate of 5 Scm³ min⁻¹ can be considered the best compromise, the efficiency is 33% with a fuel utilization of 81% and a power density of 0.600 W cm⁻² at a current density of 1.20 A cm⁻² at 0.520 V.

The limit of the procedure used to value the efficiency of a fuel cell can be the way the fuel utilization is calculated. In fact the expression used does not take into count the internal and fuel crossover current caused by leakage and electronic conductivity between the anode and the cathode.

For solid oxide fuel cells these values are generally negligible; in the case of the GDC electrolyte the electronic conductivity is not negligible, causing a difference between the theoretical and

real value. In order to realize the fuel utilization factor, it will be necessary to conduct a gas chromatography analysis of the outlet gas of the fuel cell in order to determine the real percentage of hydrogen converted in the cell (this analysis is out of the scope of this study).

4. Conclusions

In this paper, the electrochemical performance of an anode supported micro-tubular solid oxide fuel cell fed by hydrogen has been investigated. The micro-tubular SOFC used is anode supported, consisting of a NiO and Gd_{0.2}Ce_{0.8}O_{2-x} (GDC) cermet anode, a thin GDC electrolyte, and a La_{0.6}Sr_{0.4}Co_{0.2}Fe_{0.8}O_{3-y} (LSCF) and GDC cermet cathode. The cells were fed by hydrogen and the polarization curves were calculated for different values of the operating temperature and fuel flow. Results showed that the cell under investigation is dramatically sensitive to its operating temperature. Similarly, the selection of the appropriate value of the fuel flow is necessary in order to achieve good values of electrical efficiency, fuel utilization factor and power density. The results of the parametric study presented in this paper showed that the values of 550 °C and 2 Scm³ m⁻¹, respectively, for the operating temperature and fuel flow, can be considered as the optimal values according to the above mentioned criteria. In addition, results also showed that the cell under investigation is capable of achieving very high values of power density, significantly decreasing cell capital costs. On the other hand, the electrical efficiency must be significantly increased in order to be competitive with existing SOFC Technology. Therefore, additional experiments will be performed changing the SOFC materials, aiming at reducing ohmic losses. Future developments of this study will also include the possibility of using different fuels (such as natural gas, biogas, syngas, etc) in order to evaluate the corresponding thermodynamic and electrochemical performances.

References

- [1] Y. Funahashi, T. Shimamori, T. Suzuki, Y. Fujishiro, M. Awano, Journal of Power Sources 163 (2007) 731–736.
- [2] M.C. Williams, J.P. Strakey, W.A. Surdoval, L.C. Wilson, Solid State Ionics 177 (2006) 2039.
- [3] M. Mori, H. Yoshiko, N.M. Sammes, Solid State Ionics 135 (2000) 743.
- [4] J. Turner, M.C. Williams, K. Rajeshwar, Electrochemical Society Interface 13-3 (2004) 24.

- [5] K. Kendall, M. Palin, *Journal of Power Sources* 71 (1998) 268.
- [6] X. Zhou, J. Ma, F. Deng, G. Meng, X. Liu, *Journal of Power Sources* 162 (2006) 279.
- [7] S. Livermore, J. Cotton, R. Ormerod, *Journal of Power Sources* 86 (2000) 411.
- [8] U.B. Pal, S. Gopalan, W. Gong, 2004. FY 2004 Annual Report, Office of Fossil Energy Fuel Cell Program, 262.
- [9] J. Pusz, A. Mohammadi, N. Sammes, *ASME Journal of Fuel Cell Science and Technology* 3 (4) (2006) 482–486.
- [10] N.M. Sammes, Y. Du, R. Bove, *Journal of Power Sources* 145 (2005) 428.
- [11] T. Suzuki, T. Yamaguchi, Y. Fujishiro, M. Awano, *Journal of Power Sources* 160 (2006) 73.
- [12] T. Suzuki, T. Yamaguchi, Y. Fujishiro, M. Awano, *Journal of Electrochemical Society* 153 (2006) A925.